Competition between magnetism and superconductivity in $CeCu_2Si_2$

R. Feyerherm* and A. Amato
Institute for Particle Physics, ETH Zürich, CH-5232 Villigen PSI, Switzerland

C. Geibel
Institut für Festkörperphysik, TH Darmstadt, 64289 Darmstadt, Germany

F. N. Gygax
Institute for Particle Physics, ETH Zürich, CH-5232 Villigen PSI, Switzerland

P. Hellmann
Institut für Festkörperphysik, TH Darmstadt, 64289 Darmstadt, Germany

R. H. Heffner
Los Alamos National Laboratory, Los Alamos, New Mexico 87545

D. E. MacLaughlin
University of California, Riverside, California 92521-0413

R. Müller-Reisener
Institut für Festkörperphysik, TH Darmstadt, 64289 Darmstadt, Germany

G. J. Nieuwenhuys
Kamerlingh Onnes Laboratory, Leiden University, 2300 RA Leiden, The Netherlands

A. Schenck
Institute for Particle Physics, ETH Zürich, CH-5232 Villigen PSI, Switzerland

F. Steglich
Institut für Festkörperphysik, TH Darmstadt, 64289 Darmstadt, Germany
(Received 26 December 1996; revised manuscript received 7 March 1997)

The interplay between superconductivity and magnetism in $CeCu_2Si_2$ has been investigated by means of microprobe, muon spin rotation and relaxation (μSR), and specific-heat measurements on four slightly off-stoichiometric polycrystalline samples $Ce_{1+x}Cu_{2+y}Si_2$. Microprobe analysis reveals that within the errors ($\pm 3\%$) the main phases of all four samples exhibit the ideal stoichiometry 1:2:2 and their relative composition varies by less than 2%. Muon spin rotation and relaxation measurements, however, reveal pronounced differences in their ground states. The nonsuperconducting sample $Ce_{0.99}Cu_{2.02}Si_2$ exhibits a phase transition at $T_m = 0.67$ K to a magnetically ordered ground state of unknown structure, with a lower limit on the size of the frozen moments $\mu \approx 0.2\mu_B$. For $T < T_m$ slow residual fluctuations of these moments at a rate $\nu \approx 3$ MHz are observed. In the three superconducting samples comparable magnetic behavior is found in reduced volume fractions. Paramagnetic and magnetic regions are distributed inhomogeneously in these samples, the relative volume fractions being strongly sample and temperature dependent. In all samples considerable volume fractions remain magnetic down to $T = 60$ mK. The present data provide evidence that superconductivity sets in first in the paramagnetic regions, and, on further cooling, reduces the magnetically ordered volume fraction. Superconductivity and magnetic order do not appear to spatially coexist, but compete in $CeCu_2Si_2$. [S0163-1829(97)03126-3]

I. INTRODUCTION

The heavy-fermion superconductors are a small class of cerium- or uranium-based intermetallic compounds (for recent reviews see Refs. 1–3), which despite their low superconducting transition temperatures $T_c \leqslant 2$ K attract considerable and continued interest. This arises from the fact that in these compounds the interaction of the more or less localized f electrons with the conduction electrons appears to be the prerequisite for the occurrence of superconductivity. In all other classes of superconductors, the pair-breaking effect of the magnetic f ions leads to a more or less pronounced reduction of T_c or even to complete suppression of superconductivity (e.g., Refs. 4 and 5).

The keys to an understanding of the heavy-fermion superconductors are the characteristic properties of the low-

temperature state from which the superconductivity evolves. Heavy-fermion behavior is observed in many Ce-, Yb-, and U-based intermetallics. Already in systems in which the corresponding ions are dilute, an antiferromagnetic exchange interaction J between the conduction electrons and the localized f electrons may lead to a dynamical screening of the f electrons by a spin-polarized cloud of conduction electrons below a characteristic temperature T_K, resulting in the well-known Kondo effect. In compounds in which the f ions are arranged periodically—the so-called Kondo lattices—the on-site Kondo interaction competes with the intersite magnetic Rudermann-Kittel-Kasuya-Yosida (RKKY) interaction, both determined by the same J. In Doniach's Kondo-necklace model[6,7] this gives rise to a phase diagram in which a magnetic-nonmagnetic transition is encountered at a critical value J_c.

Beyond J_c coherence effects may lead to a new type of ground state, i.e., the formation of a band of quasiparticles with ''Fermi temperatures'' of $T^* \simeq 1-100$ K, closely related to T_K. Ideally, the thermodynamic and transport properties of this band show Fermi-liquid behavior and the quasiparticles can be characterized by large effective masses of $m^* \simeq (10-1000)m_0$ (for a recent review on the theory see Ref. 8).

A superconducting ground state of a Kondo lattice was first discovered in $CeCu_2Si_2$ ($T_c \simeq 0.6$ K).[9] Besides $CeCu_2Si_2$, five uranium-based compounds are considered as heavy-fermion superconductors (at ambient pressure) to date. Recently, the compounds $CeCu_2Ge_2$,[10] $CePd_2Si_2$,[11] and $CeRh_2Si_2$,[12] which are isostructural to $CeCu_2Si_2$, have been found to become superconducting under pressure.

In all heavy-fermion superconductors the Cooper pairs form out of a system of quasiparticles with strongly enhanced effective mass. Heavy-fermion superconductivity therefore is thought to occur close to the magnetic-nonmagnetic transition of the Kondo lattices. In this picture, it is facilitated by the screening of the f-electron magnetic degrees of freedom and favored by the simultaneous increase of the density of states at the Fermi surface. In this context, one of the most important subjects remains the coexistence and possible interplay of superconductivity and magnetic ordering in all of these systems except pure UBe_{13}. In the other uranium-based heavy-fermion superconductors antiferromagnetic ordering with $T_N \gg T_c$ is found. In UPd_2Al_3 magnetic ordering of *localized* $5f$ magnetic moments coexists with heavy-fermion superconductivity.[13,14] The fact that both collective ground states are governed by the same f electrons appears to imply a contradiction with the Kondo-lattice picture discussed above and raises questions about the applicability of this widely used model on these systems.[15] It is important to note at this point that in contrast to the heavy-fermion superconductors, in all other classes of magnetic superconductors magnetism and superconductivity are carried by different, comparatively weakly interacting electron systems.

First evidence for a phase transition of magnetic origin in $CeCu_2Si_2$ at 0.6 K was found in magnetoresistivity,[16] nuclear magnetic resonance (NMR),[17] and muon spin rotation and relaxation (μSR) experiments.[18] Subsequently, a B-T phase diagram has been established in which the superconducting phase lies embedded in a magnetic one (see Ref. 19 and references therein). However, the nature of the magnetic phase, i.e., the magnetic structure and the spin dynamics, has not been clarified to date.

In the present work we wish to give a detailed account of μSR measurements performed on several polycrystalline samples with different nominal compositions $Ce_{1+x}Cu_{2+y}Si_2$. This work is an extension of systematic studies of polycrystalline samples of varying stoichiometry by resistivity, specific-heat, and thermal expansion measurements.[20] These studies are aimed at a systematic study of the composition dependence of the magnetic and superconducting properties. Preliminary accounts of these studies have been published earlier.[21,22] In parallel to our work, independent μSR measurements have been carried out by a group at Columbia University.[23]

The central result of these investigations is that superconductivity and magnetism do not appear to coexist on a microscopic scale but rather compete in $CeCu_2Si_2$. In several samples suppression of magnetic ordering on the onset of superconductivity has been found, a behavior which has never been observed before in any other superconductor.

This article is organized as follows. After a brief description of the experimental details (Sec. II), we shall summarize some macroscopic properties of the investigated samples (Sec. III). We will then present the experimental results of the μSR measurements in the paramagnetic state and the low-temperature phases in Sec. VI. A discussion follows in Sec. V.

II. EXPERIMENTAL PROCEDURE

Four polycrystalline samples of different nominal composition $Ce_{1+x}Cu_{2+y}Si_2$ were prepared by melting the corresponding amounts of the elements in a triarc furnace. The samples were annealed for 48 h at 700 °C and for 72 h at 1000 °C. Pieces of these samples were used for x-ray diffraction and measurements of the specific heat and other macroscopic properties. The superconducting transition temperatures have been determined by ac-susceptibility and resistivity measurements. Electron probe microanalysis (EPMA) has been carried out at the Kamerlingh Onnes Laboratory, Leiden.

The polycrystalline samples, consisting of several slices of $1-1.5$ mm thickness and 8 mm diameter, were glued onto pure silver sample holders. The low-temperature μSR measurements ($T \leqslant 1.25$ K) were carried out at the Low-Temperature Facility (LTF) and the measurements at higher temperatures at the General-Purpose Spectrometer (GPS), both located on the πM3 beam line of the Paul Scherrer Institute, Villigen, Switzerland. The sample holders were attached to the cold finger of either a ^{3}He-^{4}He dilution refrigerator (LTF) or a continuous-flow ^{4}He cryostat (GPS).

III. SAMPLES

Some properties of the four samples are listed in Table I. The specific-heat and thermal-expansion data of the sample Nos. 1, 2, and 4 have already been published.[20] Specific-heat results on sample No. 4 in magnetic field and under pressure have been reported in Ref. 15. Specific-heat data on sample No. 1 in an external magnetic field have been published in

TABLE I. Compositions of the polycrystalline samples under investigation. ''Nominal'' compositions are before melting. The EPMA results are given for the main phase and precipitates. The superconducting transition temperatures are given in the last column. The labeling of the samples is identical to the one used in Refs. 20 and 22.

	Nominal Ce:Cu:Si	EPMA[a] vol. %, Ce:Cu:Si	T_c (K)
No. 1	1 : 2.05 : 2	>95%, 1 : 1.99 : 1.97 <5%, 0.03 : 3.62 : 1	0.69
No. 2	1 : 2.20 : 2	≈95%, 1 : 2.02 : 1.97 ≈5%, 0.06 : 16.3 : 1	0.59
No. 3	1.025 : 2 : 2 (= 1:1.95:1.95)	≈95%, 1 : 2.03 : 1.96 ≈5%, 1 : 0.64 : 1.33	0.55
No. 4	0.99 : 2.02 : 2 (= 1:2.04:2.02)	>97%, 1 : 1.99 : 1.99 <3%, 0.02 : 3.3 : 1	[b]

[a]Absolute accuracy 3%, relative accuracy 1%.

[b]Onset of superconductivity seen only in ac susceptibility at 0.45 K. From the bulk properties (see text and Ref. 20) it is concluded that the sample is not a bulk superconductor.

Ref. 24. This sample is identical to the sample used for NMR experiments.[25,26]

The nominal stoichiometry (the composition before melting) of the four samples is listed in Table I together with the results of the EPMA. Besides the main phase, small amounts ($\leqslant 5\%$ vol.) of secondary phases were observed in all samples. Within the errors of the EPMA ($<\pm 3\%$ absolute) in all four samples the main phase exhibits the ideal Ce:Cu:Si stoichiometry of 1:2:2. Their relative stoichiometry varies by less than 2%. The inhomogeneity of the composition within the main phases of the present samples is $\leqslant 1\%$. The composition of the secondary phases varies from sample to sample. In the samples prepared with Cu excess (Nos. 1, 2, and 4) the precipitates are Cu rich and practically free of Ce. The average composition of the secondary phase in sample No. 3 is compatible with the observation of 3% $Ce_2Cu_{1+x}Si_{3-x}$ by x-ray diffraction. The lattice parameters [$a=4.4002(4)$ Å, $c=9.919(1)$ Å at ambient T] are equal in all samples.

In spite of the similar compositions of the main phases, the four samples exhibit pronounced differences in their low-temperature specific heat, which is shown as C/T in Fig. 4(a). Comparison of these data with the specific-heat jump observed in an ''ideal'' superconducting single crystal[27] and the specific-heat coefficient observed in $B>B_{c2}$, i.e., in the normal state,[28] already suggests the presence of different superconducting volume fractions in the four samples. A quantitative determination, however, is difficult on the basis of the specific-heat data alone.

The superconducting transition temperatures T_c of each sample are also given in Table I. From the absence of a strong anomaly in the specific-heat coefficient in sample No. 4, together with its weak field dependence[15] and the behavior of the thermal expansion,[20] which is comparable with that of nonsuperconducting single crystal,[27] it is concluded that superconductivity in this sample appears only in minor parts of the sample volume.

IV. RESULTS

Muon spin rotation or relaxation (μSR) spectroscopy is a powerful tool for the study of weak magnetic phenomena. For a review on μSR studies in heavy-fermion compounds see Ref. 29. For details on the μSR technique we refer the reader to Refs. 30 and 31.

In the present work we make use of the sensitivity of μSR in zero applied field to weak internal magnetic fields. This sensitivity arises from the large gyromagnetic ratio of the muon, $\gamma_\mu/2\pi=135.54$ MHz/T. As a spin-1/2 particle, however, the μ^+ has no electric quadrupole moment and therefore is insensitive to electrostatic quadrupolar interactions. The internal fields are either of electronic origin or are caused by the nuclear magnetic moments of the host lattice atoms. The nuclear dipole fields are usually static in the time window of μSR (fluctuation times $T_2 \geqslant 10^{-4}$ s), while the electronic magnetic fields may be of static or dynamic nature.

The time evolution of the normalized polarization $G(t)$ [$G(0)=1$] of the muon ensemble implanted into the sample depends on the average value, distribution, and time evolution of the internal fields, and therefore contains all the physics of the magnetic interactions of the μ^+. $G(t)$ corresponds to the free induction decay signal in NMR or the signal in γ-γ-perturbed correlations. The possible presence of different μ^+-stopping sites or of regions with different ground states may be identified by different components in the depolarization function $G(t)$, $G(t)=\Sigma a_i G_i(t)$. In the case of different domains the relative amplitudes $a_i(\Sigma a_i=1)$ of the different components are a measure of the associated volume fractions.

A. Zero-field results in the normal state

Zero-field (ZF) μSR measurements have been carried out on sample Nos. 1 and 3 for 2.5 K and for 5 K and on sample No. 2 ($Ce_{2.2}Cu_2Si_2$) at 10 K$\leqslant T\leqslant$200 K. In all three samples a slow Gaussian depolarization is observed in the investigated temperature range. For example, Fig. 1(a) shows the time dependence of the normalized polarization $G(t)$ in sample No. 1 at 2.5 K. The depolarization is too slow for the possible recovery of the μ^+ polarization to $G(t\rightarrow\infty)=1/3$ [see below, Eq. (3)] to be observed within the time window of the present experiment. We therefore fitted the Gaussian approximation

$$G_{\rm pm}(t)=\exp(-\Delta_{\rm pm}^2 t^2) \tag{1}$$

to the data, where the subscript (pm) denotes the paramagnetic state. The temperature dependence of $\Delta_{\rm pm}$ observed in sample No. 2 is shown in Fig. 1(b). For temperatures 10 K $<T<$100 K, $\Delta_{\rm pm}$ is approximately constant, with a slight tendency to decrease at higher temperatures. The extrapolated value of $\Delta_{\rm pm}(T\rightarrow 0)=0.135(5)\,\mu{\rm s}^{-1}$ is the same as the values observed in sample Nos. 1 and 3 at 2.5 K. For $T>100$ K the depolarization rate exhibits a more pronounced decrease, apparently reflecting motional narrowing due to the onset of μ^+ diffusion, with a very small hopping rate of

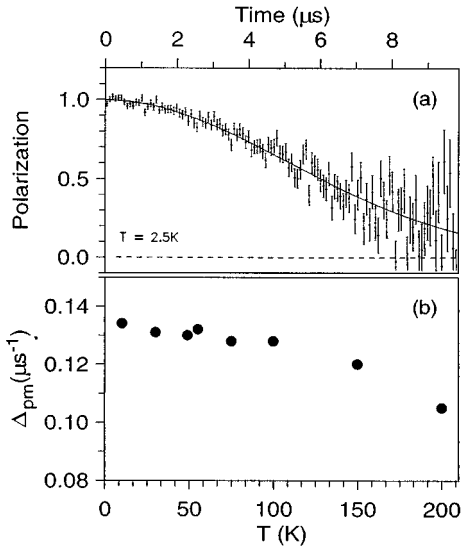

FIG. 1. (a) Time dependence of the normalized polarization $G(t)$ in sample No. 1 in zero field at $T=2.5$ K. The curve is a fit to a Gaussian, yielding $\Delta_{pm}=0.135(5)\ \mu s^{-1}$. (b) Temperature dependence of the zero-field depolarization rate Δ_{pm} (from fits of a Gaussian) in sample No. 2 ($CeCu_{2.2}Si_2$).

$\nu \ll 0.1$ MHz at 200 K. We assume that the muon is static for $T \leqslant 10$ K. Longitudinal field measurements on sample No. 3 in a 50 mT field at 0.7 K indicate that at this temperature there is no significant contribution from fluctuating electronic moments to the depolarization rate (for details see below). Therefore, we assume that the depolarization observed for $T \geqslant 2.5$ K is caused solely by the nuclear dipole fields. The observed depolarization rate corresponds to a width of the Gaussian magnetic field distribution $\Delta B=0.22$ mT at the muon site. (For a disussion of the μ^+ stopping site in $CeCu_2Si_2$, see the Appendix.)

B. Zero-field results in the low-temperature phases

In the following we present the results of μSR measurements in the temperature region $0.06\ \text{K} \leqslant T \leqslant 1.25$ K on the four $Ce_{1+x}Cu_{2+y}Si_2$ samples. First we will discuss the μSR spectra obtained in ZF experiments, in which the magnetic phase is identified. We then present additional LF measurements on sample No. 3 which help to establish the quasistatic nature of the magnetic state. In addition, TF measurements in sample No. 3 are shown which prove that the entire nonmagnetic volume fraction becomes superconducting.

The time dependence of the muon polarization $G(t)$ observed in all four samples at different temperatures is shown in Fig. 2. The $G(t)$ data on sample No. 4 ($Ce_{0.99}Cu_{2.02}Si_2$) are very similar to previous results on a $CeCu_{2.1}Si_2$ sample,[18] whereas the data on sample No. 1 ($CeCu_{2.05}Si_2$) compare well with results on a $CeCu_{2.2}Si_2$ sample.[23] A comparison of the different data sets reveals strong sample dependences.

At 1.1 K, $G(t)$ is dominated by the slow Gaussian depolarization observed at higher temperatures. To describe this signal we apply the Gaussian function [Eq. (1)]. The depolarization rates Δ_{pm} observed in the different samples for

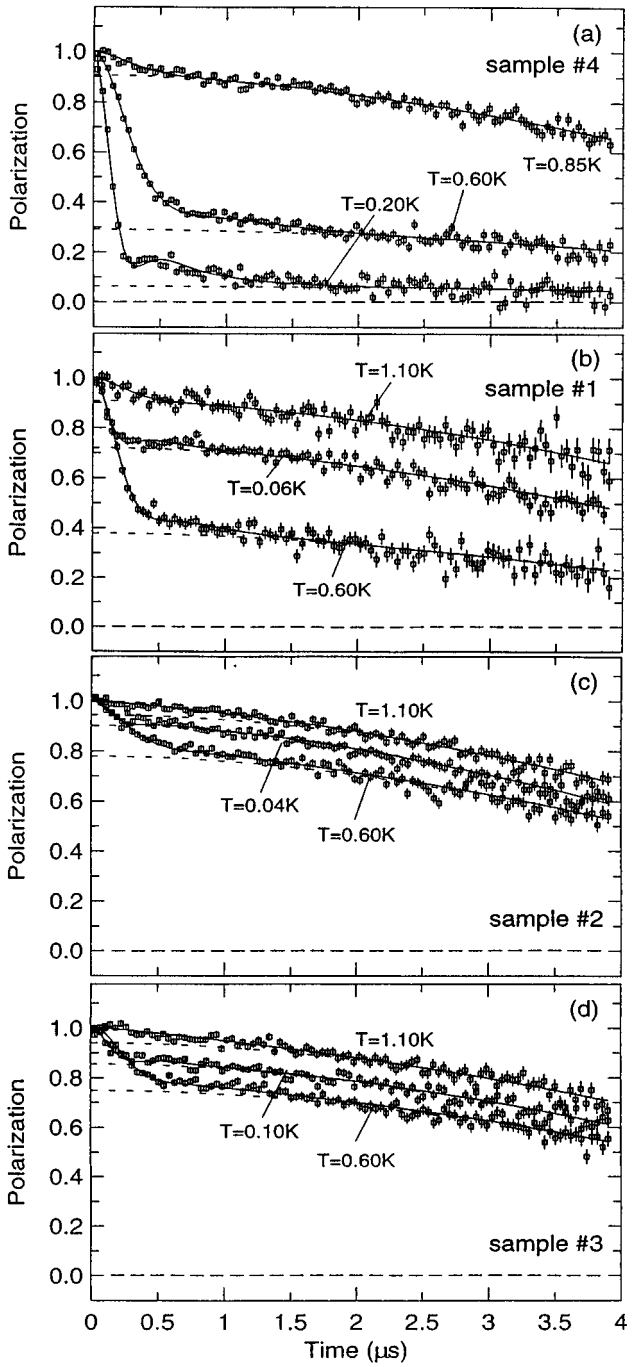

FIG. 2. Time dependence of the normalized muon polarization $G(t)$ at different temperatures: (a) in sample No. 4, (b) in sample No. 1, (c) in sample No. 2, and (d) in sample No. 3. Note the pronounced two-component structure of $G(t)$, which is composed of a slowly (dashed curve) and a rapidly depolarizing component, corresponding to paramagnetic and magnetic domains, respectively. For the fits to the data marked as solid lines see text.

$T=1.1$ K in the paramagnetic phase are in the range $\Delta_{pm}=0.135-0.150\ \mu s^{-1}$, in good agreement with the values observed at higher T.

In all samples, a fast depolarizing component appears around 1 K (see the behavior at early times in Figs. 2(a)–2(d)]. The magnitude of the corresponding depolarization rate implies the occurrence of magnetic fields of electronic

origin at the μ^+ sites, which point to quasistatic correlations between the $4f$ electrons of the Ce^{3+} ions (i.e., the $4f$ spin fluctuations are very slow compared to the paramagnetic state, where fluctuation times are typically of order $10^{-10}-10^{-14}$ s).

The clear two-component structure in $G(t)$ shows that only a fraction of the implanted muons exhibit a fast depolarization at $T\simeq 1$ K. Since the muon is a local probe, this implies the presence of two different μ^+ environments. A fraction of the implanted muons resides in an environment exhibiting practically static magnetic correlations between the Ce $4f$ ions, whereas the other muons are localized in a paramagnetic environment. This behavior indicates a spatial separation of magnetic and paramagnetic regions.

The amplitude of the fast component, which is a direct measure of the magnetic volume fraction, increases rapidly with decreasing temperature to a maximum at about $0.6-0.7$ K in sample Nos. 1, 2, and 3, followed by a significant decrease at lower temperatures. Clearly, all samples exhibit an inhomogeneous behavior at all temperatures below $T<1.2$ K, with the coexistence of magnetic and paramagnetic domains. The magnetic volume fractions are strongly sample and temperature dependent. It should be pointed out that this behavior excludes an interpretation of the two-components of $G(t)$ in terms of the occupancy of two different μ^+ stopping sites.

We analyze the $G(t)$ data by fitting a two component depolarization function

$$G(t)=a_{\rm pm}G_{\rm pm}(t)+a_{\rm m}G_{\rm m}(t) \tag{2}$$

to the time spectra with $G_{\rm pm}(t)$ given above [Eq. (1)] and $a_{\rm pm}+a_{\rm m}=1$. The amplitudes $a_{\rm pm}$ and $a_{\rm m}$ are a direct measure of the volume fractions of paramagnetic and magnetic regions, respectively. The choice of the depolarization function $G_{\rm m}(t)$ for the description of the fast depolarizing signal is not straightforward. Since the behavior of the nonbulk superconducting sample No. 4 is dominated by the fast component at $T<0.6$ K, the analysis of these data is carried out first.

In sample No. 4 [see Fig. 2(a)] the initial shape of the fast depolarizing signal is Gaussian at all temperatures. The rapid Gaussian depolarization shows that the implanted muons experience a wide range of internal fields. In addition, in all spectra recorded at $T\leqslant 0.55$ K, the polarization drops to a minimum, followed by a partial recovery at longer times and by a subsequent complete loss of polarization of the fast component at $t>2$ μs (see the spectrum for $T=0.20$ K). This shape of the depolarization function was not reported in previous μSR works. It implies a depolarization of the average 1/3 component of the initial muon polarization which would be oriented parallel to the internal magnetic fields in the static case. Thus, the observed behavior is indicative of slow dynamical fluctuations of the internal magnetic fields at the μ^+ site even at the lowest temperatures.

Such a time dependence of the polarization is usually described by the so-called dynamical Kubo-Toyabe function $G_{\rm KT}^{\rm dyn}(t)$. This function is a generalization of the static Kubo-Toyabe function[32]

$$G_{\rm KT}(t)=\frac{1}{3}+\frac{2}{3}(1-\Delta^2t^2)\exp\left(-\frac{1}{2}\Delta^2t^2\right), \tag{3}$$

which results from an isotropic Gaussian distribution of internal fields centered at zero field,

$$f(B_i)\propto\exp\left(-\frac{\gamma_\mu^2B_i^2}{2\Delta^2}\right). \tag{4}$$

Here $i=x,y,z$ and $2\Delta^2/\gamma_\mu^2=\langle B_i^2\rangle=\Delta B$ represents the second moment of the field distribution. The initial time dependence of $G_{\rm KT}(t)$ is Gaussian,

$$G_{\rm KT}(t)\simeq\exp(-\Delta^2t^2) \quad \text{at} \quad t<\Delta^{-1}. \tag{5}$$

$G_{\rm KT}(t)$ exhibits a minimum at $t\simeq 2\Delta$ and recovers to 1/3 for $t\to\infty$.

The dynamical Kubo-Toyabe function $G_{\rm KT}^{\rm dyn}(t)$ results from a Gaussian field distribution given by Eq. (4) fluctuating in time at a rate ν. With the exception of some limiting cases, it cannot be expressed analytically. It can, however, be calculated numerically using the strong collision model.[33] For slow fluctuations ($\nu<\Delta$), $G(t)$ still exhibits a minimum, but the $\frac{1}{3}$ component of Eq. (3) now also shows relaxation, and $G(t\to\infty)=0$. For $\nu\approx\Delta$, the initial depolarization is still Gaussian, but $G(t)$ drops monotoneously to zero. These two cases we are encountering in $CeCu_2Si_2$. Therefore, for the description of the rapidly depolarizing signal we use

$$G_{\rm m}(t)=G_{\rm KT}^{\rm dyn}(\Delta_{\rm m},\nu,t), \tag{6}$$

where $\Delta_{\rm m}$ and ν correspond to the width of the field distribution ($\Delta B=\sqrt{2}\Delta_{\rm m}/\gamma_\mu$) and the fluctuation rate of the internal fields, respectively. We obtain good fits to the experimental data, using Eqs. (1), (2), and (6), as demonstrated in Fig. 2(a). Note that for $T\geqslant 0.6$ K the minimum in the time dependence of the polarization vanishes. For $T\geqslant 0.75$ K convergence problems appear in fitting to Eq. (6), caused by the small amplitude $a_{\rm m}$ and the lack of structure in the rapidly depolarizing signal. In this case the exact shape of the experimental depolarization function $G_{\rm m}(t)$ is masked by the statistical errors and is therefore not well determined. To solve this problem, we made use of the observation (to be discussed in detail below) that in the region $T\leqslant 0.75$ K an approximately constant fluctuation rate ν is observed. For the fits to the data at higher temperatures we have therefore fixed ν to its corresponding average value.

The fitted results for the temperature dependence of the amplitude $a_{\rm m}$, corresponding to the volume fraction of the magnetically correlated regions, are shown in Fig. 3(a). Clearly $a_{\rm m}$ exhibits a broadened transition centered at $\langle T_{\rm m}\rangle=0.66$ K. The half-width of the transition is $\Delta T_{\rm m}=0.08$ K. For $T\leqslant 0.5$ K less than 10% of the volume of the sample is paramagnetic. At least part of this volume corresponds to the Cu-rich precipitates (see Sec. III).

Figure 3(b) shows the temperature dependence of $\Delta_{\rm m}$ and the fluctuation rate ν for the magnetic volume fraction. The value of $\Delta_{\rm m}$ is a measure of the magnetic order parameter. Its temperature dependence roughly follows the behavior usually observed for a continuous magnetic phase transition. However, because of the broad inhomogeneous distribution of magnetic transition temperatures in the present sample, a quantitative discussion is difficult. The extrapolation yields a value $\Delta B(T\to 0)=11$ mT, consistent with earlier results[18,23] on other samples. Most important, the fluctuation rate ν is

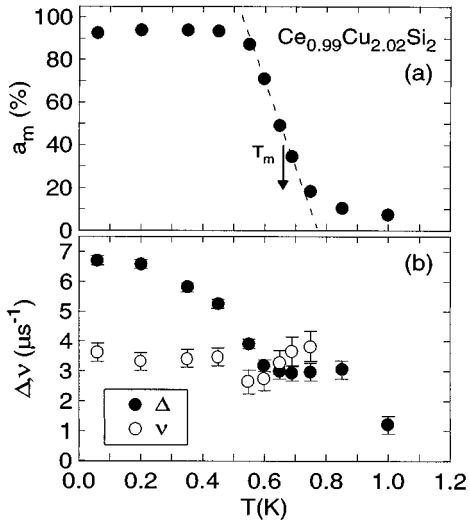

FIG. 3. (a) Temperature dependence of the relative amplitude a_m of the rapidly relaxing component in sample No. 4, corresponding to the volume fraction of the magnetic regions. The curve is a guide to the eye. (b) Temperature dependence of the parameter Δ_m (solid symbols) and of the fluctuation rate ν (open symbols), obtained from the fit of Eqs. (2) and (6) to the experimental $G(t)$ data. Note that all values describe only the *magnetic* volume fraction at a given temperature. For $T \geqslant 0.75$ K the value of ν was fixed to 3.2 MHz in the fits.

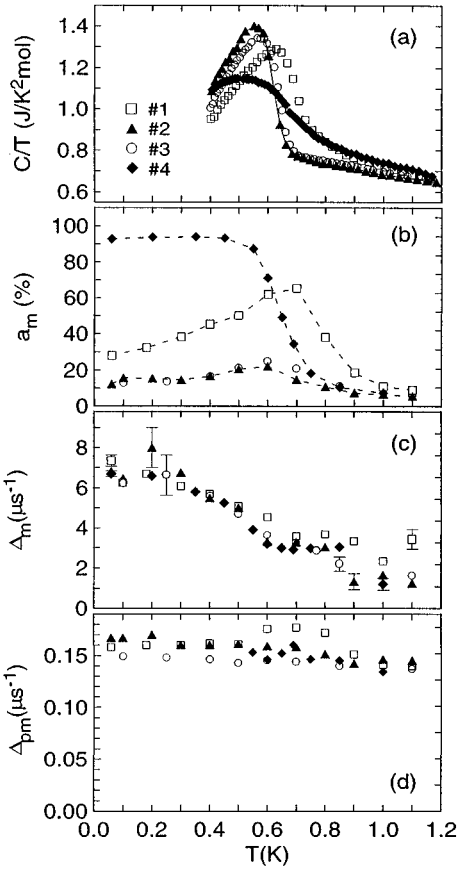

FIG. 4. Temperature dependence of (a) the specific heat coefficient C/T, (b) the relative intensity a_m of the fast relaxing component, corresponding to the volume fraction of magnetic domains, (c) the depolarization rate Δ_m in these domains, and (d) the depolarization rate Δ_{pm} in the paramagnetic domains in all four samples under investigation.

virtually temperature independent, with an average value of 3.2 MHz for $T < 0.75$ K. The crossover from $\nu < \Delta$ to $\nu \geqslant \Delta$ is the reason for the disappearance of the minimum in the time dependence of $G_m(t)$ for $T \geqslant 0.6$ K; see Fig. 2(a).

As discussed above, the magnetic regions appear to be spatially separated from the paramagnetic ones in the three superconducting specimens. We are interested mainly in the determination of the magnetic volume fractions and in a comparison of the magnetic properties in the different samples.

Due to the reduced amplitude of the fast depolarizing signal $G_m(t)$ in the three superconducting samples [see Figs. 2(b)–2(d)], the application of the dynamical Kubo-Toyabe fit function encounters problems. The characteristic structure in the time spectra observed for $T \leqslant 0.55$ K in sample No. 4 has too small an amplitude to be identified in the other samples. Therefore (with the exception of sample No. 2 around 0.6 K) it is impossible to obtain reliable values for the fluctuation rate in these fits. In our previous publication,[22] a Gaussian was fitted to the $G(t)$ data: $G(t) = \exp(-\Delta^2 t^2)$. In the case of a nonzero fluctuation rate this approximation to the dynamical Kubo-Toyabe function does not describe the dynamical depolarization of the 1/3 component of the signal properly. In addition, it leads to an underestimate of the width of the underlying magnetic field distribution ΔB.

We believe that a better approach is to assume that the fluctuation rates are of approximately the same magnitude in all four samples. Indeed, very similar behavior of $G(t)$ is observed in the sample Nos. 1 and 4 at $T = 0.6$ K, i.e., in the critical region, where the crossover from $\nu < \Delta$ to $\nu \geqslant \Delta$ takes place. A fit to the $G(t)$ data of sample No. 1 at $T = 0.6$ K (where the amplitude of the magnetic signal is relatively large) using the dynamical Kubo-Toyabe function yields $\nu = 3.5(3)$ MHz. We therefore used the same fit function as above [Eqs. (1), (2), and (6)], fixing the parameter ν to the average value obtained above in the fully magnetic sample No. 4, $\nu = 3.2$ MHz. A comparison between the fit results obtained with the Gaussian approximation and with the dynamical Kubo-Toyabe fit function shows that the latter is a better description of the data. The corresponding results are shown in Figs. 4(b)–4(d) together with the results of sample No. 4, already discussed.[35] (We wish to note that the present analysis yields only quantitive differences to the results published in the previous publication.[22] The central qualitative conclusions remain unchanged.)

Figure 4(b) shows the temperature dependences of the amplitudes a_m, i.e., the magnetic volume fractions in all four samples. Clearly, the superconducting samples exhibit a pronounced inhomogeneous behavior over the whole temperature range, with the coexistence of magnetic and paramagnetic regions, the magnetic volume fraction being strongly temperature and sample dependent. Most significantly, the increase of the magnetic volume fraction on cooling down from $T = 1.2$ K stops exactly at the respective superconducting transition temperatures T_c in each sample (see Table I). Below T_c, the magnetic volume fraction decreases, implying a transition back to a nonmagnetic state at lower T in a

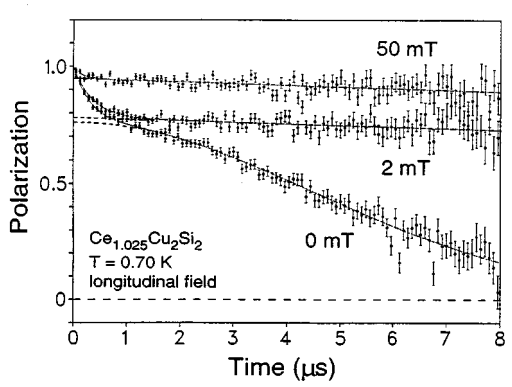

FIG. 5. Time dependence of the normalized μ^+ polarization $G(t)$ in sample No. 3 in the normal conducting state in zero and longitudinal field. Note the pronounced two-component structure of $G(t)$, which is composed of a slowly (dashed curve) and a fast depolarizing component, corresponding to paramagnetic and magnetic domains, respectively.

certain volume fraction of previously magnetic regions. This effect is most pronounced in sample No. 1.

Concerning the nature of the magnetic phase in the four samples under investigation, we may compare the depolarization rates Δ_m of the corresponding fast signals [see Fig. 4(c)]. The observed temperature dependence is very similar, suggesting equal magnetic states in all four samples. The values of Δ_{m} increase continuously on cooling, unaffected by the superconducting transition, even while the magnetic volume fraction decreases. (Again, a quantitative discussion of the temperature dependence of Δ_{m} is difficult because of the strongly inhomogeneous behavior and the temperature-dependent magnetic volume fractions in each sample.)

The ZF depolarization rates Δ_{pm} in the paramagnetic volume fraction [Fig. 4(d)] vary slightly with temperature, $\Delta_{\mathrm{pm}}=0.14-0.18\,\mu\mathrm{s}^{-1}$ in the different samples. No significant correlation of the depolarization rate with the magnetic or the superconducting transition is observed. The origin of the observed increase of Δ_{pm} is unclear. It could point to some additional depolarization caused by fast spin fluctuations in the paramagnetic phase at the lowest temperatures.

C. Longitudinal field results

In addition to a ZF measurement, longitudinal-field (LF) measurements have been carried out on sample No. 3 at $T=0.70$ K in fields of $B=2$ mT and $B=50$ mT. The three resulting normalized asymmetry spectra $G(t)$ are shown in Fig. 5.

The ZF result is well described by Eq. (2) with the dominant component from the paramagnetic volume fraction described by a Gaussian function with $\Delta_{\mathrm{pm}}=0.14(1)\ \mu\mathrm{s}^{-1}$. The fast depolarizing component at this temperature is best described by an exponential $G_{\mathrm{m}}(t)=\exp(-\lambda_{\mathrm{m}}t)$, with $\lambda_{\mathrm{m}}=3\ \mu\mathrm{s}^{-1}$. This shape is in contrast to the Gaussian behavior observed in sample No. 4. However, the depolarization rate λ_{m} is comparable to the value of Δ_{m} observed in sample No. 4. Therefore, the exponential shape is presumably produced by an approximately Lorentzian shape of the underlying field distribution (with a half-width of $\Delta B_{\mathrm{m}}\approx 5$ mT) instead of by faster spin fluctuations in sample No. 3.

In a LF of $B=2$ mT, which meets the relation $\Delta B_{\mathrm{pm}}<B<\Delta B_{\mathrm{m}}$, the depolarization of the signal from the paramagnetic volume is strongly reduced, while $G_{\mathrm{m}}(t)$ is only slightly affected. However, the paramagnetic signal continues to exhibit a very slow residual depolarization. Fitting an exponential $\exp(-\lambda_{\mathrm{pm}}t)$ to this signal results in a depolarization rate $\lambda_{\mathrm{pm}}=0.01\ \mu\mathrm{s}^{-1}$ (which is actually at the lower detection limit of μSR). This value is rather small compared to $\Delta_{\mathrm{pm}}=0.14\ \mu\mathrm{s}^{-1}$ observed in zero field and reflects a small contribution from fast fluctuating moments in the paramagnetic state.

In a LF of 50 mT the depolarization of the fast depolarizing component is almost completely suppressed. Only a small residual rapidly depolarizing signal is observed. Such a behavior is theoretically expected for the present case, where $B\simeq\Delta B_{\mathrm{m}}$.[30] The results are in agreement with the finding of only a very slow fluctuation on the MHz scale in the ZF measurements.

D. Transverse-field results

Transverse-field (TF) measurements after field cooling (FC) have been carried out on sample No. 3 at $T=0.1-1$ K in a field of 50 mT. To account for the paramagnetic and the magnetic volume fractions, as well as the sample holder signal, a three-component function was fitted to the asymmetry spectra:

$$\begin{aligned} AG(t)=A_{\mathrm{sample}}\{&a_{\mathrm{m}}\exp(-\sigma_{\mathrm{m}}^2t^2/2)\cos\omega_{\mathrm{m}}t\\ &+a_{\mathrm{pm}}\exp(-\sigma_{\mathrm{pm}}^2t^2/2)\cos\omega_{\mathrm{pm}}t\}\\ &+A_{\mathrm{holder}}\cos(\omega_{\mathrm{holder}}t), \end{aligned} \tag{7}$$

where $\omega_i=2\pi\nu_i$. The signals from the sample holder and the paramagnetic fraction cannot be resolved at the small field of $B=50$ mT, while the signal from the magnetic volume fraction is distinguished by its large depolarization rate σ_{m}.

The ratio A_{holder}/A was therefore determined in a TF measurement at $B=1$ T at $T=0.7$ K. This measurement also yielded an estimation of the average Knight shift, $K\simeq(\omega_{\mathrm{m,pm}}/\omega_{\mathrm{holder}})-1\simeq-7\times10^{-3}$.

The ratio A_{holder}/A was assumed to be field independent and the value of A_{holder} was fixed in the fits to the low-field spectra. In addition we set $\omega=\omega_{\mathrm{m}}=\omega_{\mathrm{pm}}$, because the frequencies of the signals are not resolved. The results of these fits for a_{m} and σ_{m} are shown in Fig. 6. They are in good agreement with the corresponding ZF data on the magnetic volume fraction in sample No. 3 [compare Fig. 4(b) and 4(c)].

To check whether the whole paramagnetic volume fraction becomes superconducting at T_c we performed zero-field-cooling (ZFC) TF measurements ($B=20$ mT) on sample No. 3 at 0.4 K$\leqslant T\leqslant$0.7 K. Above T_c, the dominant signal from the paramagnetic phase exhibits a slow depolarization comparable to the FC value. Below T_c, the ZFC procedure, i.e., increasing the field from zero to a field larger the lower critical field [$B_{c1}=2.3$ mT (Ref. 38)], is expected to produce a wide magnetic field distribution in superconducting regions because of pinning of the flux lines and a correspondingly distorted vortex lattice.

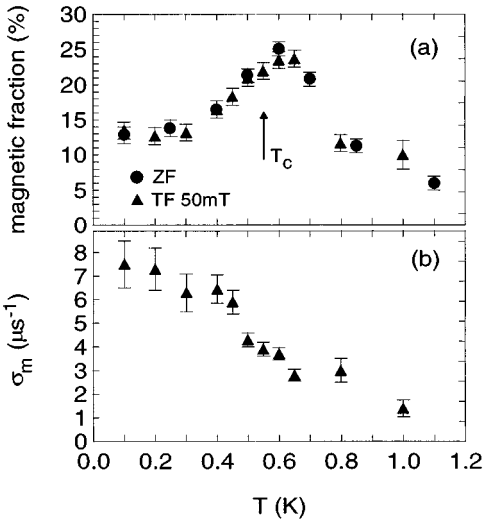

FIG. 6. (a) Temperature dependence of the relative intensity a_m of the fast relaxing component in sample No. 3, determined in the field-cooling TF measurements at $B=50$ mT (open squares), together with the results from the zero-field measurements (solid circles). (b) The temperature dependence of the field-cooling TF depolarization rate σ_m in the magnetic domains in sample No. 3, defined by Eq. (7).

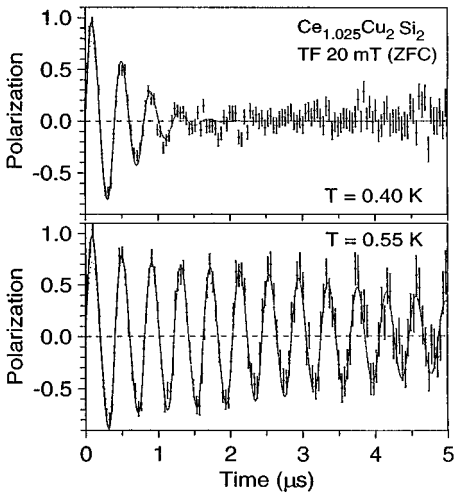

FIG. 7. Time dependence of the normalized asymmetry $G(t)$ at different temperatures in sample No. 3 in a transverse field of 20 mT after zero-field cooling from $T>T_c$. Upper figure: $T<T_c$. Lower figure: $T\simeq T_c$. A small signal from the sample holder has been subtracted from the data.

The normalized asymmetry spectra $G(t)$ obtained in these ZFC-TF measurements were fitted with Eq. (7). To allow for a separate description of the signals from the magnetic and the paramagnetic regions also below T_c, the parameters a_m and σ_m were fixed to their values determined in the FC measurements at 50 mT. It has to be noted that in doing this we assume that the μ^+ depolarization in the magnetic regions is not influenced by the flux line lattice. The present data do not allow us to prove this assumption, due to the large depolarization rates in both kinds of regions.

Two representative spectra obtained above and below T_c are presented in Fig. 7. (The small signal from the sample holder has been subtracted from the data.) A very fast depolarization of the entire signal is indeed observed in all spectra below T_c, which proves that in the full paramagnetic volume fraction (including the ''reentrant'' paramagnetic fraction) a wide field distribution is induced by the ZFC procedure. This observation is in agreement with the behavior of a $CeCu_{2.2}Si_2$ sample at $T=0.05$ K (see Ref. 23). It suggests that indeed the full paramagnetic volume becomes superconducting (in the present case, at least at 0.40 K$\leqslant T\leqslant T_c$). This implies that even the volume fraction that is magnetic at T_c, and becomes paramagnetic on further cooling, is superconducting and that no third type of region (nonsuperconducting paramagnetic) exists.

In addition to the above results, from the temperature dependence of the depolarization rate $\sigma_{pm,ZFC}$ an independent determination of the transition temperature is possible from the extrapolation $\sigma_{pm,ZFC}\rightarrow\sigma_{pm,FC}$ at $T\rightarrow T_c$. This yields $T_c=0.56$ K in sample No. 3, in good agreement with the results from measurements of bulk properties.

V. DISCUSSION

The occurrence of magnetic ordering in $CeCu_2Si_2$ is not surprising in view of the results of recent systematic studies of the series $CeCu_2(Ge_{1-x}Si_x)_2$.[39,40] There, it was observed that on increasing Si doping x the magnetic transition temperature in $CeCu_2Ge_2$ ($T_N=4.15$ K) is gradually suppressed, extrapolating to 0.7 K for $x\rightarrow 1$. Neutron scattering[40] reveals that the incommensurate magnetic structures are similar for $0\leqslant x\leqslant 0.4$ but the ordered moment is significantly reduced by Si doping. For Si concentrations $x>0.4$ the ordered moment is too small to be detected. In these studies it appears that the magnetic ordering observed in $CeCu_2Si_2$ might be closely related to that in $CeCu_2Ge_2$.

The observation in sample No. 4 ($Ce_{0.99}Cu_{2.02}Si_2$) of an inhomogeneous distribution of transition temperatures $T_m=(0.66\pm 0.08)$ K is in agreement with the previously reported onset temperature of magnetism $T_{m,onset}=0.8$ K (Ref. 18) and the values $T_m=0.63-0.67$ K reported in Refs. 19 and 27. New information on the nature of the magnetic state results from the observed slow dynamical fluctuations of the internal magnetic fields at the muon site. Since the μ^+ does not diffuse at the lowest temperatures, this points to residual electronic spin-fluctuations with $\nu\simeq 3$ MHz of the $4f$ magnetic moments below T_m. This is consistent with the ''more or less dynamic nature'' of the magnetic state reported in NMR measurements on the present sample No. 1 and other $CeCu_{2+x}Si_2$ samples,[25,26,36] where a gradual loss of the spin-echo amplitude has been observed below ≈ 1 K. Our estimate of the fluctuation rate is consistent with the estimate of $\nu\approx 0.1-10$ MHz from the NMR results.[37]

The residual fluctuations are very slow compared to the fluctuation rates in the paramagnetic state which in general are $\nu=10^{10}-10^{14}$ Hz. Therefore, one may speak of a nearly frozen, ''quasistatic'' arrangement of the $4f$ magnetic moments of the Ce^{3+} ions below T_m. It is important to stress that we do not observe a gradual slowing down of spin fluctuations near the magnetic transition, but a spontaneous freezing of the moments in certain regions, as proven by the temperature independent behavior of ν below T_m.

As argued before,[18,23] one possible spin arrangement producing the observed broad Gaussian field distribution is a dense spin-glass-like state, produced by a large density of randomly oriented magnetic moments. Such a spin arrangement, however, appears to require frustration, which cannot be of geometrical origin in the present tetragonal lattice of Ce^{3+} magnetic moments. Since precursor effects like critical slowing down of spin fluctuations at $T > T_m$ are absent in the present case, we think that a spin-glass type of ordering in $CeCu_2Si_2$ seems rather unlikely.

It has been argued that in $CeCu_2Si_2$ heavy-fermion band magnetism may be realized.[41] However, the apparent Gaussian shape of the magnetic field distribution is not compatible with any kind of highly ordered spin structures. An incommensurate spin-density-wave-type ordering, as is realized in $CeCu_2Ge_2$, is expected to produce a field distribution $f(B)$ with a characteristic peak at finite B. This leads to several oscillations in the time dependence of $G(t)$ before complete depolarization, in contrast to the observation.

Another possibility that has not been discussed to date is the presence of a commensurate antiferromagnetic structure superposed by a disorder-induced staggering of the spin arrangement. The highly ordered component of the resulting spin arrangement could (accidentally) produce canceling internal magnetic fields at a highly symmetric interstitial site, as is the supposed μ^+ site (0,0,1/2) (see the Appendix for a discussion of the μ^+-stopping site in $CeCu_2Si_2$). In that case, the μ^+ would be sensitive only to the deviations of the actual spin arrangements from the ideal structure that may appear as ''spin-glass like.'' These could arise, for example, from a possible short-range nature of the magnetic state. However, the exact nature of the magnetic state cannot be clarified on the basis of the present results.

An estimate of the size of the disordered staggered components of the magnetic moments from the observed width of $\Delta B = 11$ mT yields $0.2\mu_B$ [assuming the μ^+ site (0,0, 1/2)]. Note that this value is a lower limit for the size of the actually frozen magnetic moments. The nonobservation of magnetic Bragg peaks[42,43] appears to rule out a long-range-ordered magnetic structure with a moment of that size in $CeCu_2Si_2$.

The most important result of the present measurements on the superconducting samples $Ce_{1+x}Cu_{2+y}Si_2$ is the observation of a spatial separation of magnetic and paramagnetic regions in all samples. We would like to stress that the quantitative determination of different volume fractions and their temperature dependence in $CeCu_2Si_2$ has only be accomplished by μSR to date. The size of the different regions cannot be determined by μSR. However, it seems reasonable to assume that a given crystallite within the polycrystalline sample behaves homogeneously. In sample Nos. 2 and 3 the crystallite structure could be observed in the EPMA electron backscattering photographs, showing an average crystallite diameter of about 30 μm.

The present μSR data on the temperature dependence of the magnetic volume fractions strongly suggest that superconductivity sets in first in the entire paramagnetic volume and prevents the development of magnetism in these regions. There is no direct proof from the μSR data that the magnetic regions are not superconducting. Evidence for normal conducting behavior in the magnetic regions, however, stems from the comparison of the temperature dependence of the magnetic volume fractions observed in the μSR data with the corresponding behavior of the specific heat of our four samples (see Fig. 4).

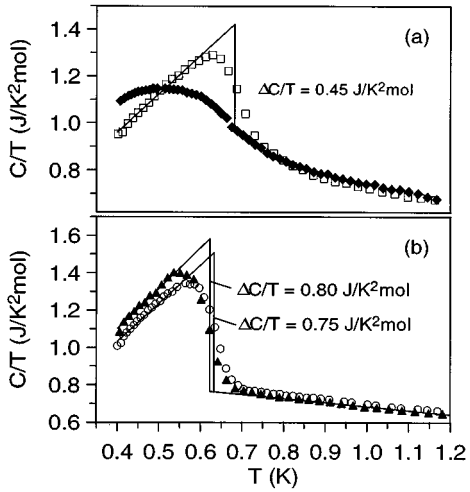

FIG. 8. Temperature dependence of the specific heat coefficient C/T in (a) sample Nos. 2 and 3 and (b) sample Nos. 1 and 4 [same data as in Fig. 4(a)]. The idealized specific-heat jumps using the entropy balance are indicated. For details, see text.

As discussed in Sec. III, the behavior of the specific heat in sample No. 4 points to only a very small superconducting volume fraction. The specific heat [see Fig. 4(a)] is enhanced as compared to the values for good superconducting samples in the temperature range $0.6 < T < 1.2$ K in sample No. 4. This additional contribution is independent of magnetic field up to the superconducting upper critical field $B_{c2} = 2$ T.[24] It reflects the broadened magnetic transition observed in the μSR measurements.

In sample No. 1 the paramagnetic volume fraction at T_c, determined by μSR, is about 30%. Here, the specific heat exhibits an intermediate behavior. At $T > 0.7$ K it closely follows the temperature dependence observed in sample No. 4, reflecting magnetic ordering in a large volume fraction. The superconducting transition at $T_c = 0.7$ K is reflected in a rather small jump of C/T. Here the determination of the specific-heat jump at T_c is difficult due to the magnetic contribution. By comparison with the behavior of the completely magnetic sample, and taking into account the entropy balance we estimate a value of $\Delta C/T_c = 0.40$ J/K^2 mol in sample No. 1 [see Fig. 8(a)]. With the values of $C_n(T_c)/T_c = 0.75$ J/K^2 mol and $\Delta C/C_n = 1.48$ in an ''ideal'' superconducting single crystal[27] we estimate the superconducting volume fraction in sample No. 1 to be $(35 \pm 10)\%$.

In sample Nos. 2 and 3, the paramagnetic volume fraction at T_c, derived from the μSR data, is $\simeq 80\%$ and $\simeq 75\%$, respectively. The temperature dependence of the specific heat is close to that of the ''ideal'' superconducting single crystal, although the superconducting transitions appear somewhat broadened. By comparison with the ''ideal'' behavior we estimate superconducting volume fractions of $(75 \pm 10)\%$ in sample No. 2 and $(70 \pm 10)\%$ in sample No. 3 [see Fig. 8(b)]. Clearly, in all samples the size of the jump $\Delta C/C_n$ of the specific heat at T_c scales with the paramag-

netic volume fraction at T_c determined in the present μSR work, suggesting that superconductivity appears only in the paramagnetic regions.

The fact that magnetism and superconductivity occur in spatially separated volume fractions may be taken as an indication that these two phenomena are in competition in $CeCu_2Si_2$. The magnetically ordered state appears always to be the ground state if the superconducting state is not established. No third type of ground state (e.g., a paramagnetic, nonsuperconducting one) exists in $CeCu_2Si_2$, as argued already in Ref. 23.

Strong evidence of a competition of magnetism and superconductivity in $CeCu_2Si_2$ is the reduction of the magnetic volume fraction below T_c in the superconducting samples, which is most pronounced in sample No. 1 ($CeCu_{2.05}Si_2$). It is interpreted in terms of the suppression of magnetism by the onset of superconductivity in certain regions. At least in the corresponding volume fraction (in sample No. 1 about 40%) magnetism and superconductivity exhibit direct competition.

It is important to note that a certain magnetic volume fraction persists down to lowest T in each sample, implying that superconductivity is completely prevented in the corresponding regions. We wish to stress that the temperature dependence of the superconducting volume fraction may contribute to the specific heat below T_c and therefore may lead to an unusual temperature dependence of $C_p(T)$. We conclude that three kinds of behavior may appear in a certain region: ''S'' $T_c > T_m$, and the region becomes superconducting without showing magnetic behavior, ''AS'' $T_c < T_m$, and the region first becomes magnetic but the magnetic order is destroyed at the onset of superconductivity at a lower T. This implies that the superconducting state is more stable at $T \rightarrow 0$ than the magnetic one. Finally, ''A'' $T_c \rightarrow 0$ ($T_c \ll T_m$), and the ground state is magnetic.

These findings are in one-to-one correspondence with the classification of different polycrystalline samples and single crystals of $CeCu_2Si_2$ based on their macroscopic properties.[20,15] From our EPMA results we conclude that apparently very small variations of the main phase composition of less than 2% may alter the behavior dramatically. The inhomogeneous behavior of the polycrystalline samples under investigation shows that even an inhomogeneity less than $\pm 1\%$ is sufficient to vary the ground state.

The source of this sensitivity is unclear. It may just reflect sample quality; i.e., in the good superconducting samples the stoichiometry is closer to the ideal 1:2:2 composition than in other samples. In the latter, the superconductivity is prevented by lattice imperfections like vacancies or disorder between the different types of atoms (notably, the occupancy of the Cu sites may vary[44]).

Another approach is the idea, based on the extended Doniach model,[6,7] that superconductivity requires a minimal strength of the hybridization, corresponding to a minimal exchange interaction J between the $4f$ and conduction electrons. Superconductivity takes place only if a sufficient moment compensation by the Kondo screening is achieved. As a possible source of a sample dependence, variations of the lattice parameter a, determining the $4f-5d$ hybridization, have been considered.[27] The lattice parameters, in turn, may be influenced by internal strain.[45] This idea is supported by the observation that in the present, fully magnetic sample No. 4 the magnetic transition is suppressed by a moderate pressure of 5 kbar, being replaced by a superconducting transition at 0.6 K.[15] Similar behavior in single crystals,[46] as well as an increase of the superconducting volume in samples with a small superconducting volume fraction on application of pressure,[47] has been reported before. Moreover, this behavior is in line with the observation of an unusual increase of T_c with pressure in $CeCu_2Si_2$,[48,49] as well as the suppression of magnetic ordering with pressure in $CeCu_2Ge_2$,[10] $CePd_2Si_2$,[11] and $CeRh_2Si_2$.[12] Remarkably, in all of these compounds the onset of superconductivity is observed at the brink of magnetic ordering. Accidentally, $CeCu_2Si_2$ appears to be close to this magnetic-to-superconducting transition at ambient pressure.

The overall behavior found in the $CeCu_2Si_2$ system suggests that magnetism and superconductivity are almost degenerate, and thus competing ground states. Moreover, the destruction of magnetic order by the onset of superconductivity in the samples of type AS points to a subtle interrelation between these ground states. It is important to note that such a behavior has never been observed in any other superconductor.

The microscopic mechanism for the suppression of magnetism in the superconducting state is unclear. A possible suppression of the RKKY interaction or a more effective Kondo screening in the superconducting state have been discussed as possible sources in Ref. 23. However, we wish to note that, assuming the magnetic state in $CeCu_2Si_2$ to be of the heavy-fermion band-magnetism type, a noncoexistence of magnetic ordering and superconductivity appears quite natural. The coexistence would require a simultaneous spin pairing of the quasiparticles in the Cooper pairs and a magnetic spin alignment of the same quasiparticles.

VI. CONCLUSION

The present μSR results provide clear evidence for a competition between the superconducting state with $T_c = 0.7$ K and a magnetically ordered state. Both do not coexist on a microscopic scale in $CeCu_2Si_2$. In polycrystalline samples inhomogeneous behavior may be observed. Superconductivity takes place in paramagnetic volume fractions or suppresses magnetic ordering in certain regions. Parts of the samples investigated in the present work remain magnetic down to the lowest temperatures. The results strongly suggest that experimental data taken on polycrystalline samples should always be interpreted taking into account a possible inhomogeneity.

In the light of the extended Doniach Kondo-lattice model, the behavior of the above-mentioned cerium based heavy-fermion superconductors, including $CeCu_2Si_2$ may be taken as evidence that in these compounds the formation of (or at least closeness to) a nonmagnetic ground state is a prerequisite for appearance of superconductivity. This suggests that magnetism and superconductivity arise from competing interactions within the same set of quasiparticles forming the heavy-fermion state in these compounds. This in contrast to the behavior of U-based HFS like URu_2Si_2 or UPd_2Al_3, where magnetism and superconductivity coexist on a microscopic level. In UPd_2Al_3, several experiments suggest the

presence of two microscopically coexisting $5f$ subsystems of different kind.[13,14] This discrepancy gives rise to the question[15] whether cerium- and uranium-based heavy fermion compounds differ fundamentally in the corresponding $4f$ and $5f$ electronic states, respectively.

ACKNOWLEDGMENTS

We are indebted to S. Süllow (KOL,Leiden) and T. Gortenmulder (FOM-ALMOS center, Leiden) for the EPMA investigations. This work is partly supported by the SFB 252 Darmstadt/Frankfurt/Mainz and U.S. NSF Grant No. DMR-9114911, and was carried out in part under the auspices of the U.S. DOE.

APPENDIX

The ZF depolarization rate Δ_{pm} (see Sec. IV A) is frequently used as a source of information on the μ^+-stopping site. From the large number of interstitial sites in the $ThCr_2Si_2$ structure a set of possible μ^+ sites can be obtained by comparison of the observed zero-field depolarization rate with theoretical values Δ_{nuc} for the effect of the nuclear dipole fields from the ^{63}Cu, ^{65}Cu ($I=3/2$), and ^{29}Si ($I=1/2$) isotopes (the latter is neglected in the following because of its small abundance). We calculated the theoretical values for the polycrystalline average of Δ_{nuc} for two limiting cases. The quantization axis for the Cu nuclei is assumed to be either parallel to the radial direction towards the muon ($\Delta_{nuc,rad}$) or parallel to the c axis ($\Delta_{nuc,ax}$). These directions are determined by the possible electric field gradients experienced by the nuclei. For the corresponding theory, see Ref. 30. The expected actual depolarization rate is some intermediate value, because only nuclei very close to the muon might experience the radial electric field gradient. In Table II, all sites with theoretical values for the depolarization rate $\Delta_{nuc} \leqslant 0.25\ \mu s^{-1}$ are listed. For all of these sites the calculated values differ from the experimentally observed value by 15% or more, and thus the μ^+-stopping site cannot be identified.

TABLE II. Calculated values of the polycrystalline depolarization rate Δ_{nuc} for radial (rad) and axial (ax) electric field gradient at the Cu nuclei, for different interstitial sites in $CeCu_2Si_2$. The experimental value is $\Delta_{pm}=0.135\mu s^{-1}$.

Site	$\Delta_{nuc,rad}$ (μs^{-1})	$\Delta_{nuc,ax}$ (μs^{-1})
$2b(0,0,1/2)$	0.084	0.064
$4c(1/2,0,0)$	0.101	0.094
$4e(0,0,z)$, $z=0.20$	0.296	0.153
$z=0.25$	0.216	0.171
$8j(1/2,x,0)$, $x=0.25$	0.091	0.067

In the isostructural compound $CeRu_2Si_2$ the $2b$ site (0,0,1/2) has been identified as the μ^+-stopping site from the Knight shift anisotropy measured on a single crystal.[34] From these data, an occupation of the nonaxially symmetric sites $4c$ and $8j$ could be positively excluded. It should also be noted that the $2b$ site is the carbon site in the structurally related borocarbide superconductors. We therefore believe that the $2b$ is the most likely μ^+ site in $CeCu_2Si_2$. However, the origin of the enhancement of the experimentally observed value of Δ_{nuc} as compared to the calculated ones for the site $2b$ is unclear. An increased value of the nuclear dipole fields at the muon site could be produced by a lattice distortion in the neighborhood of the μ^+. In that case, one has to assume that the neighboring Cu atoms are displaced by more than 15% towards the muon.

*Present address: Department of Physics and Astronomy, McMaster University, Hamilton, Ontario, Canada L8S 4M1.

[1] N. Grewe and F. Steglich, in *Handbook on the Physics and Chemistry of Rare Earths*, edited by K.A. Gscheidner, Jr. and L. Eyring (North-Holland, Amsterdam, 1991), Vol. 14, p. 343.

[2] F. Steglich, U. Ahlheim, C.D. Bredl, C. Geibel, M. Lang, A. Loidl, and G. Sparn, in *Frontiers in Solid State Science*, edited by L.C. Gupta and M.S. Multani (World Scientific, Signapore, 1992), p. 527.

[3] R.H. Heffner and M.R. Norman, Comments Condens. Matter Phys. **17**, 361 (1996).

[4] Ø. Fischer, in *Handbook of Ferromagnetic Materials*, edited by K.H.J. Buschow and E.P. Wohlfahrt (Elsevier Science, Amsterdam, 1990), Vol. 5, p. 465.

[5] G. Hilscher, H. Michor, N.M. Hong, T. Holubar, W. Perthold, M. Vyboronov, and P. Rogl, Physica B **206&207**, 542 (1995).

[6] S. Doniach, Physica B **91**, 231 (1977).

[7] M.A. Continentino *et al.*, Phys. Rev. B **39**, 9734 (1989).

[8] A.C. Hewson, *The Kondo Problem to Heavy Fermions* (Cambridge University Press, Cambridge, England, 1993).

[9] F. Steglich, J. Aarts, C.D. Bredl, W. Lieke, D. Meschede, W. Franz, and J. Schäfer, Phys. Rev. Lett. **43**, 1892 (1979).

[10] D. Jaccard, K. Behnia, and J. Sierro, Phys. Lett. A **163**, 475 (1992).

[11] F.M. Grosche, S.R. Julian, N.D. Mathur, and G.G. Lonzarich, Physica B **223&224**, 50 (1996).

[12] R. Movshovich, T. Graf, D. Mandrus, M. F. Hundley, J.D. Thompson, R.A. Fisher, N.E. Phillips, and J.L. Smith, Physica B **223&224**, 126 (1996).

[13] R. Caspary, P. Hellmann, M. Keller, G. Sparn, C. Wassilew, R. Köhler, C. Geibel, C. Schank, F. Steglich, and N.E. Phillips, Phys. Rev. Lett. **71**, 2146 (1993).

[14] R. Feyerherm, A. Amato, F.N. Gygax, A. Schenck, C. Geibel, F. Steglich, N. Sato, and T. Komatsubara, Phys. Rev. Lett. **73**, 1849 (1994).

[15] F. Steglich, P. Gegenwart, C. Geibel, R. Helfrich, P. Hellmann, M. Lang, A. Link, R. Modler, G. Sparn, N. Bütgen, and A. Loidl, Physica B **223&224**, 1 (1996).

[16] U. Rauchschwalbe, F. Steglich, A. de Visser, and J.J.M. Franse, J. Magn. Magn. Mater. **63&64**, 347 (1987).

[17] H. Nakamura, Y. Kitaoka, H. Yamada, and K. Asayama, J. Magn. Magn. Mater. **76&77**, 517 (1988).

[18] Y. J. Uemura, W.J. Kossler, X.H. Yu, H.E. Schone, J.R. Kempton, C.E. Stronach, S. Barth, F.N. Gygax, B. Hitti, A. Schenck, C. Baines, W.F. Lankford, Y. Onuki, and T. Komatsubara, Physica C **153-155**, 455 (1988); Phys. Rev. B **39**, 4726 (1989).

[19] G. Bruls, B. Wolf, D. Finsterbusch, P. Thalmeier, I. Kouroudis, W. Sun, W. Assmus, B. Lüthi, M. Lang, K. Gloos, F. Steglich,

and R. Modler, Phys. Rev. Lett. **72**, 1754 (1994).
[20] R. Modler, M. Lang, C. Geibel, C. Schank, R. Müller-Reisener, P. Hellmann, A. Link, G. Sparn, W. Assmus, and F. Steglich, Physica B **206&207**, 586 (1995).
[21] A. Amato, Physica B **199&200**, 91 (1994).
[22] R. Feyerherm, A. Amato, C. Geibel, F.N. Gygax, P. Hellmann, R.H. Heffner, D.E. MacLaughlin, R. Müller-Reisener, G. Nieuwenhuys, A. Schenck, and F. Steglich, Physica B **206&207**, 596 (1995).
[23] G.M. Luke, A. Keren, K. Kojima, L.P. Le, B.J. Sternlieb, W.D. Wu, Y.J. Uemura, Y. Onuki, and T. Komatsubara, Phys. Rev. Lett. **73**, 1853 (1994); see also G.M. Luke *et al.*, Hyperfine Interact. **85**, 397 (1994).
[24] T.C. Kobayashi, A. Koda, H. Honda, K. Amaya, Y. Kitaoka, K. Asayama, C. Geibel, and F. Steglich, Physica B **206&207**, 600 (1995).
[25] Y. Kitaoka, H. Nakamura, T. Iwai, K. Asayama, U. Ahlheim, C. Geibel, C. Schank, and F. Steglich, J. Phys. Soc. Jpn. **60**, 2122 (1991).
[26] Y. Kitaoka, H. Tou, G.-q. Zheng, K. Ishida, K. Asayama, T.C. Kobayashi, A. Kohda, N. Takeshita, K. Amaya, Y. Onuki, C. Geibel, C. Schank, and F. Steglich, Physica B **223&224**, 55 (1996).
[27] M. Lang, R. Modler, U. Ahlheim, R. Helfrich, P.H.P. Reinders, and F. Steglich, Phys. Scr. **T39**, 135 (1991).
[28] F. Steglich, C.D. Bredl, W. Lieke, U. Rauchschwalbe, and G. Sparn, Physica B **126**, 82 (1984).
[29] A. Schenck, in *Frontiers in Solid State Science*, edited by L.C. Gupta and M.S. Murani (World Scientific, Singapore, 1993), Vol. 2.
[30] A. Schenck, *Muon Spin Rotation Spectroscopy* (Adam Hilger, London, 1985).
[31] J.H. Brewer, in *Encyclopedia of Applied Physics*, edited by G. L. Trigg, E. S. Vera, and W. Grenlich (VCH, New York, 1994), Vol. 11, pp. 23–53.
[32] R. Kubo and T. Toyabe, in *Magnetic Resonance and Relaxation*, edited by R. Blinc (North-Holland, Amsterdam, 1967).
[33] R.S. Hayano, Y.J. Uemura, J. Imazato, N. Nishida, T. Yamazaki, and R. Kubo, Phys. Rev. B **20**, 850 (1979).
[34] A. Amato *et al.*, PSI Newslett. 1993, Pt. 1, p. 89 and (unpublished).
[35] In certain temperature regions ($T \geqslant 0.65$ K) the present choice of the fit function does not necessarily yield the best fits to the spectra observed in sample Nos. 1, 2, and 3. The data may be sometimes better described by an exponential depolarization. However, to obtain a consistent description for the complete set of the present data, we use the dynamical Kubo-Toyabe ansatz over the whole temperature range. We checked that this procedure does not affect the results on the main parameters of interest significantly.
[36] H. Nakamura, Y. Kitaoka, T. Iwai, H. Yamada, and K. Asayama, J. Phys. Condens. Matter **4**, 473 (1992).
[37] Y. Kitaoka (private communication).
[38] U. Rauchschwalbe, W. Lieke, C.D. Bredl, F. Steglich, J. Aarts, K.M. Martini, and A.C. Mota, Phys. Rev. Lett. **49**, 1448 (1982).
[39] O. Trovarelli, M. Weiden, R. Müller-Reisner, M. Gómez-Berisso, J.G. Sereni, C. Geibel, and F. Steglich, Physica B **223&224**, 295 (1996).
[40] G. Knebel, C. Eggert, D. Engelmann, R. Viana, A. Krimmel, M. Dressel, and A. Loidl, Phys. Rev. B **53**, 11 586 (1996).
[41] F. Steglich, U. Ahlheim, C.D. Bredl, C. Geibel, A. Grauel, M. Lang, G. Sparn, A. Krimmel, A. Loidl, and W. Assmus, J. Magn. Magn. Mater. **108**, 5 (1992).
[42] S. Horn, E. Holland-Moritz, M. Loewenhaupt, F. Steglich, H. Scheuer, A. Benoit, and J. Flouquet, Phys. Rev. B **23**, 3171 (1981).
[43] E. Holland-Moritz, W. Weber, A. Severing, E. Zirngiebl, H. Spille, W. Baus, S. Horn, A.P. Murani, and J.L. Raggazoni, Phys. Rev. B **39**, 6409 (1989).
[44] H. Spille, U. Rauchschwalbe, and F. Steglich, Helv. Phys. Acta **56**, 165 (1983).
[45] W. Assmus, M. Herrmann, U. Rauchschwalbe, S. Riegel, W. Lieke, H. Spille, S. Horn, G. Weber, F. Steglich, and G. Cordier, Phys. Rev. Lett. **52**, 469 (1984).
[46] F.G. Aliev, N.B. Brandt, V.V. Moschchalkov, and S.M. Chudinov, J. Low Temp. Phys. **57**, 61 (1984).
[47] A. Bleckwedel and A. Eichler, Solid State Commun. **56**, 693 (1985).
[48] D. Jaccard, J.M. Mignot, B. Bellarbi, A. Benoit, H.F. Braun, and J. Sierro, J. Magn. Magn. Mater. **47&46**, 23 (1985).
[49] F. Thomas, J. Thomasson, C. Ayache, C. Geibel, and F. Steglich, Physica B **186-188**, 303 (1993).